Manipulation of Nanoscale Components with the AFM: Principles and Applications

A. A. G. Requicha, S. Meltzer, F. P. Terán Arce, J. H. Makaliwe,
H. Sikén, S. Hsieh, D. Lewis, B. E. Koel and M. E. Thompson

Laboratory for Molecular Robotics
University of Southern California
requicha@lipari.usc.edu

Abstract

Bottom-up construction of nanostructures from molecular-sized components is a promising approach to nanofabrication. This paper discusses bottom-up techniques that involve positioning of nanoparticles or nanorods with an Atomic Force Microscope (AFM), and, for certain applications, chemical linking of such components.

The physical principles of nanomanipulation with an AFM are described, with an emphasis on Dynamic Force Microscopy (DFM). Sources of spatial uncertainty are discussed. It is shown that nanoparticles and nanorods can be reliably positioned on a surface by pushing them with the tip of an AFM. Typical nanomanipulation operations are conducted at room temperature, in ambient air or in a liquid.

For many applications nanostructures composed of nanoparticles or nanorods must be linked together. This can be done by using self-assembling linkers or by electroless deposition. The ability to immobilize the particles on a surface also is important in some applications. Again, self-assembly techniques can be used to imbed the particles in deposited layers.

1. Introduction

The Scanning Probe Microscope (SPM) was invented in the early 1980s by Binnig and Rohrer, of the IBM Zürich Laboratory, and earned them a Nobel Prize. SPMs opened a new window into the nanoworld and have been a major force driving the current development of nanoscience and engineering. Although SPMs are normally used for imaging, it was recognized soon after their invention that they can also modify the samples. Eigler's group at the IBM Almadén Laboratory demonstrated that the Scanning Tunneling Microscope (STM) can be used to manipulate atoms [17]; a well-known example of their work is the IBM logo written with xenon atoms. Other pioneering research on atomic manipulation was done by Avouris' and Aono's groups [6, 20]. Atom manipulation is typically performed in ultra high vaccum (UHV) and at low temperature (~ 4 K).

Building nanoobjects atom by atom in UHV at 4K is not very practical. An alternative approach, pioneered by Samuelson's group at the University of Lund [5], starts with larger, molecular-sized building blocks and assembles them with an Atomic Force Microscope (AFM) in ambient conditions. Our group at USC's Laboratory for Molecular Robotics (LMR) has been investigating this approach for several years [1]. Work on AFM-based manipulation has been reported by other groups [18, 15, 16, 7, 19].

An AFM is both a sensor and a manipulator, and we do not have an independent measurement of "ground truth" when we navigate the tip over the sample. Operating the AFM in the chamber of a Scanning Electron Microscope (SEM) provides a separate sensing capability. Visual feedback from the SEM can be used for the manipulation, much like one normally does with optical microscopes at a larger scale [21]. Manipulation inside an SEM was pioneered by Sato's group [14] for microscale objects, and has been used at the nanoscale by the Ruoff/Zyvex group [23] and Fukuda's [4]. SEM sensing is not appropriate for all samples, because it normally requires a vacuum environment and involves bombarding the sample with high energy electrons. SEMs also tend to have lower resolution and be more expensive than SPMs.

In the remainder of this paper we discuss the issues that arise in using an AFM (without SEM sensing) as a robot, and review some of the results obtained at LMR.

2. DFM Robotics

2.1 Atomic Force Microscopy

The AFM is a conceptually simple apparatus [13]. A micrometer-scale cantilever with a sharp tip (diameter ~ 10-50 nm) is scanned over a sample at distances on the order of a few nm. Interatomic forces between the tip and the sample are sensed by the cantilever, whose deflection is measured (usually) by a

laser and a photodetector. The force experienced by the tip varies nonlinearly with the tip-sample separation, as shown in Figure 1.

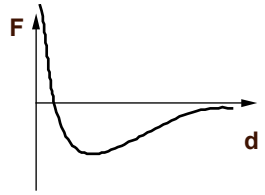

Figure 1 – Idealized force-separation curve. Positive forces are repulsive.

In *contact mode* operation, the tip is in the repulsive region of the curve, and the force is kept constant during the scan by a feedback circuit that monitors the photodetector signal. A tip in contact mode exerts a relatively large normal force on the sample, and also a substantial lateral force. As a result, fragile samples are damaged, and tips tend to wear out rapidly. In addition, the deflection signal is low-pass and the process is subject to low-frequency noise.

The preferred mode of operation often is Dynamic Force Microscopy (DFM), which uses a vibrating cantilever and avoids the force and noise problems of contact mode. There are two versions of DFM. In *non-contact mode*, the tip oscillates above the sample in the attractive force regime, whereas in *intermitent contact mode*, the tip contacts the sample for a short time interval ("taps") during each cycle of the oscillation. DFM is discussed next.

2.2 Principles of DFM Operation

First let us consider non-contact mode. An oscillating cantilever can be approximated by a point mass m attached to a spring of stiffness k, moving in a medium with coefficient of friction c, and subject to a non-linear force $F(z)$, which depends on the tip-sample separation as indicated in Figure 1. For small amplitudes, we can expand the force in Taylor series, neglect higher order terms, and linearize the equations of motion about the equilibrium. The resulting equation of motion is

$$m\,\mathrm{d}^2z/\mathrm{d}t^2 + c\,\mathrm{d}z/\mathrm{d}t + (k - \mathrm{d}F/\mathrm{d}z)\,z = 0.$$

This shows that, to a first approximation, the non-linear force has an effect equivalent to a change in the spring constant (or stiffness) of the cantilever. It follows that the resonance frequency depends on z:

$$\omega_0{}^2 = (k - \mathrm{d}F/\mathrm{d}z)/m.$$

For large values of z the interaction force $F = 0$, and the response of the cantilever to a forced excitation of frequency f_{drive} is characterized by the thick resonance curve shown in Figure 2. In the figure $f_{\mathrm{res}} = \omega_0/2\pi$ is the resonance frequency in Hz. A DFM user controls the instrument by selecting three parameters:

- the drive frequency, which typically is chosen close to resonance;
- the free amplitude, *i.e.*, the amplitude of vibration that corresponds to zero F, or large z;
- the *setpoint*, or desired amplitude of vibration A_{set}.

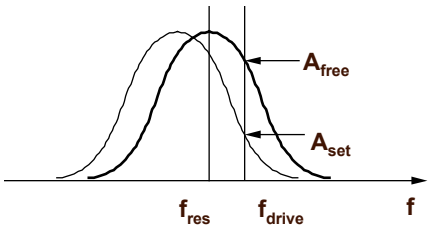

Figure 2 – DFM operation.

The AFM electronics extract the amplitude of cantilever vibration A, and a feedback circuit moves the piezo motors to ensure that $A = A_{\mathrm{set}}$. In the figure, the feedback must adjust z so that the resonance curve shifts to the left until the amplitude that corresponds to the drive frequency equals the setpoint. In essence, the feedback must search for a suitable value of the stiffness $\mathrm{d}F/\mathrm{d}z$. Therefore, scanning at a given amplitude setpoint is equivalent to keeping a constant *stiffness*, or force gradient.

This simple theory is adequate for non contact operation with small amplitudes. For intermitent contact mode the situation is more complicated, because the amplitudes are relatively large. Numerical simulation is necessary to deal with the non-linear force. Research on intermitent mode AFM is still under way, and is beyond the scope of this paper.

2.3 Imaging

The raw image produced by the AFM is an array of values $V_z(V_x, V_y)$, where the V denote voltages applied to the piezo drives responsible for motion in the x, y and z directions. In the ideal situation, in which the tip is a dimensionless point and the piezos are perfectly linear, the image faithfully reproduces the surface $z(x, y)$. Here x, y, z are piezo displacements. Recall that in DFM imaging the sample height does not necessarily equal the z piezo displacement. We showed in the previous section that, to a first order, the image is a contour of constant *stiffness*, not constant height. Therefore, even with ideal piezos, the so-called topographic image does not represent the true height of the sample. If the sample is relatively homogeneous and therefore the force-separation curve is approximately constant across the sample, there is an approximate one-to-one relationship between tip-sample separation and force gradient in stable

operation. The topographic image is then qualitatively correct but the z scale may be distorted. Non-linearity arises because of the force-separation curves, even for perfect piezos.

We will have more to say about the relationship between motion (extension) and voltage for piezos. For now we note that one can compute average, or approximate conversion factors from Volts to nm by measuring known samples. For example, x and y calibrations can be done using a crystaline surface whose lattice constant is known. For z calibration, samples with atomic steps are appropriate. Colloidal particles with known diameters (measured with an SEM, for example) are also convenient for z calibration. Note that z calibration in DFM will not give the true piezo conversion factor because of the influence of the force-separation curve. Contact mode will provide better results in this regard.

The only truly reliable way of measuring x, y, z is by using feedback. This is the approach taken in machine tools and robots in the macroscopic world. Position feedback is used in some AFMs for large scans and features. For example, some commercial instruments offer 100 µm scanners with feedback-controlled x, y positioning. Note, however, that a typical 256x256 pixel image with a scan size of 100 µm has a resolution or pixel size of ~ 400 nm, which is quite large. For the work done in our lab, scan sizes are usually < 1 µm and accuracies ~ 1 nm are required. Unfortunately, sensors and feedback circuits cannot normally offer such accuracies. Hence, commercial instruments are operated open loop for small scan sizes.

2.4 Manipulation

2.4.1 Tip Positioning

Let us now look at the AFM operating in DFM as a manipulator, rather than as a sensor. Ignoring the high frequency vibration, the tip in its DC or average position can be considered a mobile robot with 3 degrees of freedom, x, y, z. The simplest robotic command one can think of is MoveTo(x, y, z). For small scan sizes, the x, y motion will be open loop and subject to the uncertainties discussed below. But in z we can use feedback, with the cantilever (plus the photodiode and associated optics) as a sensor. However, we cannot command directly a z value; instead we must select suitable values for the DFM parameters. The crucial issue is the relationship between A_{set} and z, for fixed A_{free} and f_{drive}. This can be determined experimentally by the following procedure, which is based on the fact that the tip vibration is quenched when the DC position of the tip approaches a surface. This has been demonstrated experimentally and predicted by non-linear simulations using the oscillator model – see *e.g.* [3].

First measure the height of a spherical nanoparticle by using standard non-contact AFM with a given A_{set}. Then turn off the feedback and move towards the center of the particle. Monitor the cantilever vibration amplitude to ensure that it goes to zero, and measure the maximum DC deflection of the cantilever, which will occur at the highest point of the particle. Then $z = H - D$ as shown in Figure 3. The operating parameters must be chosen so that the particle does not move, and the amplitude decreases to zero. This approach only works for values of A_{set} below the particle's height. Note that the height H is measured in z piezo Volts and the cantilever deflection D, often called the "A – B signal", in photodetector Volts. To obtain the z displacement in nm we need to convert the piezo V into nm, as explained in the previous section, and we also need a conversion factor between photodiode voltage and cantilever deflection. This latter can be estimated by the following techniques.

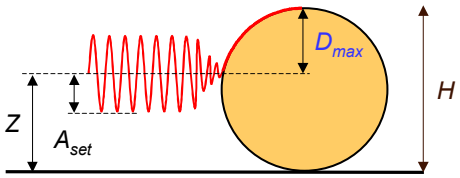

Figure 3 – Measuring the DC position of the cantilever.

The standard method for calibrating the photodiode is to push the tip against a hard surface and compare the z displacement of the piezo with the cantilever deflection measured as the output of the photodiode. They should be equal. Unfortunately, in our lab this procedure invariably ruins the sharp tips that we need to use for successful nanomanipulation. An alternative and gentler approach consists of executing a line scan over the centers of two nanoparticles of known but different heights. As shown in Figure 4, we can write $z = H_2 - cV_2 = H_1 - cV_1$ and therefore the conversion factor c can be calculated as $c = (H_2 - H_1)/(V_2 - V_1)$.

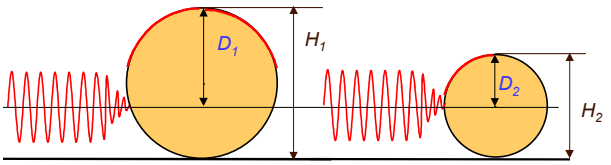

Figure 4 – Calibrating the photodiode.

2.4.2 Pushing

Nanoscale objects such as nanoparticles can be pushed mechanically by the tip of an AFM. There are several protocols for manipulation by pushing, all of which share the following aspects. First image the sample to determine where is the desired particle. Then move against the particle, but change the operating parameters so that a force higher than that used for imaging is applied. In our lab we usually push by imaging in DFM and then moving with the feedback off along a line that goes through the center of the particle. We observe that the amplitude goes to zero, the DC cantilever deflection becomes non-zero, and the particle moves, if the deflection is above a certain threshold, which depends on the cantilever and various other characteristics of the setup [11].

2.5 Sample Preparation

Imaging and manipulation with an AFM depend on the relative magnitudes of the forces between tip, objects and substrate. For example, if the attractive forces between objects and substrate are small, imaging is impossible because the objects move unpredictably when the tip interacts with them; if the forces are large, the objects do not move. Sample preparation techniques must therefore ensure that forces are in a suitable range. This is done by careful selection of the substrate surface and coatings (for the substrate and sometimes the objects), and of deposition procedures. Typically the objects are in solution and a drop is deposited on the substrate. (Specific details are given in the literature.)

In our lab, substrates are usually mica, oxidized silicon or glass. They are easy to obtain and they are flat at the nanoscale, which is an important requirement. Objects typically are colloidal gold particles or rods – see Figure 5 for a recent nanorod manipulation example.

The Au particles usually have a Cl coating which renders them negative. If we deposited them directly on mica, which also is negative when freshly cleaved, they would not adhere sufficiently for imaging. We introduce an additional layer of poly-L-lysine, which is positive and serves to anchor the Cl-cappped particles. Other useful anchoring layers are composed of silanes such as APTS or APTES, which also provide positive charges for attachment. In some cases, we prefer to use covalent bonding rather than the electrostatic interactions just described. For example the Au rods of Figure 5, which are obtained in an organic solution and are not charged, are attached to Si by using a thiolated layer. The sulfur end groups of the layer bond covalently to the Au.

In summary, sample preparation is very important and requires substantial knowledge of Chemistry, to select appropriate particle coatings and anchoring layers, and to optimize the deposition procedures and obtain uniform and flat layers.

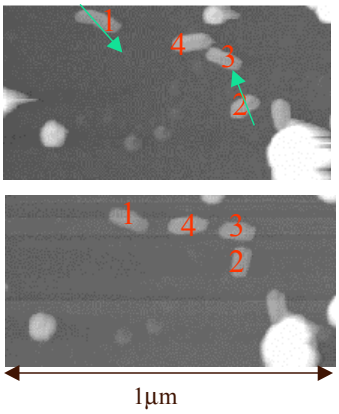

Figure 5 – Manipulation of Au nanorods, approximately 100x10 nm. Original position (top) and final position (bottom).

3. Spatial Uncertainty

There are many sources of spatial uncertainty in AFM manipulation, which we will discuss briefly in this section.

Tip Effects – When the tip moves in contact with a sample it traverses a contact manifold in configuration space. Therefore, we obtain the image of the c-space obstacle that corresponds to the sample rather than the image of the sample itself. For a discussion of tip effects and their compensation see *e.g.* [22].

Drift - The major cause of spatial uncertainty in our lab is thermal drift between the tip and the sample. We work at room temperature, in ambient air and without careful temperature and humidity control. A typical value for drift velocity is 0.05 nm/s. This implies that for an image with 256x256 pixels obtained in a 1 Hz scan an object will drift by ~ 12.5 nm, which is approximately the size of the particles we usually manipulate. If we ignored the drift, the manipulation would fail very often. Figure 6 shows two scans with a top-to-bottom fast scan direction and a left-to-right slow-scan direction in the left image, and right-to-left in the right image. The drift in the vertical direction is evident in the lower left corner of the images.

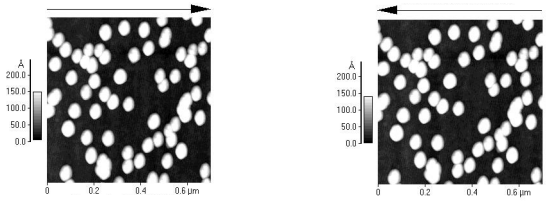

Figure 6 – Two scans of 15 nm Au nanoparticles. The scan size is 700 nm, the scanning frequency 1 Hz and the resolution 256x256.

Creep – A large voltage step will produce a rapid displacement of the tip followed by a slow creeping motion, which can last several minutes. Figure 7 illustrates this effect by imaging a small region after the scanner was offset by 1000 nm. The four images are taken at 12 sec intervals, at 20 Hz, with a scan size of 200 nm and resolution 64x64. Over a 40 sec interval creep values can reach 50 nm for a 1000 nm offset.

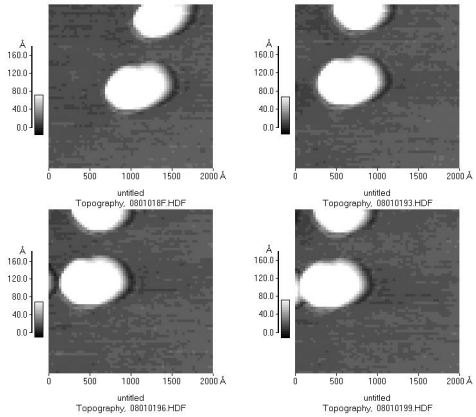

Figure 7 – Sequence of images showing creep.

Hysteresis – The extension of a piezo depends on the history of the voltages applied to it. For example, scanning right-to-left or left-to-right produces different results. The differences can be large. For example, for a 500 nm scan one can find a displacement of ~ 15 nm, which is comparable to our particle sizes.

Other Nonlinearities – Even ignoring hysteresis the piezo's response is not linear with the voltage. Therefore the V/nm conversion factor is not constant and must be calculated for different conditions. In additon, the tube scanners used in most AFMs move approximately in a circle and not in a straight line.

The spatial uncertainty that results from the sources described above causes major difficulties in manipulation of nm-scale objects, which require high resolution and hence small scan sizes and open-loop operation. Interactive nanomanipulation can rely on imaging to sense a particle's position immediately before it is moved, and therefore can finesse some of these problems. However, automatic manipulation must address them. In our lab we can compensate for drift by tracking particles, but techniques and strategies for dealing with the other nonlinearities are still under study.

4. Linking and Embedding

Patterns of unlinked nanoparticles can be useful for certain applications such as high-density data storage [2] and single-electron electronics. However, many applications require nanostructures of specific shapes. These can be approximated by groups of suitably positioned and *linked* nanoparticles. We have investigated two approaches to linking. The first uses covalent bonding to a linker [9]. For example, Au particles can be connected with di-thiols. The di-thiols self-assemble to the gold and serve as chemical glue. We have demonstrated two variants of this approach: (i) first deposit the particles, position them and then immerse the sample in the di-thiols; or (ii) deposit the particles, apply the thiols and then manipulate.

The second approach to linking also uses self-assembly: additional material is selectively deposited on the particles but not on the remainder of the sample. For example, we have shown that a pattern of Au nanoparticles can be used as a template for the electroless deposition of additional Au. Gold wires of arbitrary geometry can be built in this manner [8].

For certain applications we may need to ensure that nanocomponents are fixed on the substrate. This can also be done by selective self-assembly. Now we need a material that will assemble to the substrate but not the particles, and thus will embed the particles in a thin layer. We have demonstrated particle embedding in a silicon oxide layer by first depositing a monolayer of a silane and then oxidizing it [12]. We have used embedding of particles in successive layers for a new rapid prototyping technique at the nanoscale [10].

5. Summary and Conclusions

The AFM operating in DFM, which is usually the preferred mode of operation, behaves as a very nonlinear system. The relevant calibration factors depend on the operating conditions and are difficult to estimate accurately. Spatial uncertainty arises from many sources and is sufficiently large to cause frequent failures in manipulation operations for nanoscale objects, which require high resolution and small scan sizes. Successful manipulation can be accomplished with a human in the loop by using the AFM as a sensor, but it tends to be tedious and time consuming.

Nanomanipulation with the AFM, together with linking and immobilizing techniques, provide an evolving set of tools for constructing nanostructures from molecular-sized components. Widespread use of these tools, however, will require further advances on automation of nanomanipulation procedures.

Acknowledgements

This research was supported in part by the Z. A. Kaprielian Technology Innovation Fund and the National Science Foundation under grant EIA-98-71775.

References

[1] C. Baur *et al*., "Robotic nanomanipulation with a scanning probe microscope in a networked computing environment", *J. Vacuum Science & Technology B*, Vol. 15, No. 4, pp. 1577-1580, July/August 1997.

[2] C. Baur *et al*., "Nanoparticle manipulation by mechanical pushing: underlying phenomena and real-time monitoring", *Nanotechnology*, Vol. 9, No. 4, pp. 360-364, December 1998.

[3] A. Bugacov *et al.*, "Measuring the tip-sample separation in dynamic force microscopy", *Probe Microscopy*, Vol. 1, pp. 345-354, 1999.

[4] L. Dong, F. Arai and T. Fukuda, "3D nanorobotic manipulation of multi-walled carbon nanotubes", *Proc. IEEE Int'l Conf. on Robotics & Automation*, Seoul, S. Korea, pp. 632-637, May 21-26, 2001.

[5] T. Junno, K. Deppert, L. Montelius and L. Samuelson, "Controlled manipulation of nanoparticles with an atomic force microscope", *Applied Physics Letters*, Vol. 66, No. 26, pp. 3627-3629, June 26, 1995.

[6] I.-W. Lyo and P. Avouris, "Field-induced nanometer- to atomic-scale manipulation of silicon surfaces with the STM", *Science*, Vol. 253, No. 5016, pp. 173-176, July 12, 1991.

[7] M. Martin *et al*., "Manipulation of Ag nanoparticles utilizing noncontact atomic force microscopy", *Applied Physics Letters*, Vol. 73, No. 11, pp. 1505-1507, September 14, 1998.

[8] S. Meltzer *et al*., "Fabrication of nanostructures by hydroxylamine-seeding of gold nanoparticle templates", *Langmuir*, Vol. 17, No. 5, pp. 1713-1718, March 6, 2001.

[9] A. A. G. Requicha *et al.*, "Towards hierarchical nanoassembly", *Proc. Int'l Conf. on Intelligent Robots & Systems (IROS '99)*, Kyongju, S. Korea, pp. 889-893, October 17-21, 1999.

[10] A. A. G. Requicha *et al*., "Layered nanoassembly of three-dimensional structures", *Proc. IEEE Int'l Conf. on Robotics & Automation*, Seoul, S. Korea, pp. 3408-3411, May 21-26, 2001.

[11] R. Resch *et al.*, "Manipulation of nanoparticles using dynamic force microscopy: simulation and experiments", *Applied Physics A*, Vol. 67, No. 3, pp. 265-271, September 1998.

[12] R. Resch *et al*., "Immobilizing Au nanoparticles on SiO_2 surfaces using ODS monolayers", *Langmuir*, in press.

[13] S. Sarid, *Scanning Force Microscopy*. Oxford, U.K.: Oxford University Press, 1994.

[14] T. Sato, T. Kameya, H. Miyazaki and Y. Hatamura, "Hand-eye system in the nano manipulation world", *Proc. IEEE Int'l Conf. on Robotics & Automation*, Nagoya, Japan, pp. 59-66, 1995.

[15] D. M. Schaefer, R. Reifenberger, A. Patil and R. P. Andres, "Fabrication of two-dimensional arrays of nanometer-size clusters with the atomic force microscope", *Applied Physics Letters*, Vol. 66, No. 8, pp. 1012-1014, February 20, 1995.

[16] M. Sitti and H. Hashimoto, "Tele-Nanorobotics Using Atomic Force Microscope", *Proc. of the IEEE/RSJ Int. Conf. on Intelligent Robots and Systems, IROS'98*, Victoria, Canada, pp. 1739-1746, October 1998.

[17] J. A. Stroscio and D. M. Eigler, "Atomic and molecular manipulation with the scanning tunneling microscope", *Science*, Vol. 254, No. 5036, pp. 1319-1326, November 29, 1991.

[18] R. M. Taylor *et al*., "The nanomanipulator: a virtual reality interface for a scanning tunneling microscope", Proc. ACM SIGGRAPH '93, Anaheim, CA, pp. 127-134, August 1-6, 1993

[19] L. Theil Hansen *et al.*, "A technique for positioning nanoparticles using an atomic force microscope", *Nanotechnology*, Vol. 9, No. 4, pp. 337-342, December 1998.

[20] H. Uchida, D. H. Huang, J. Yoshinobu and M. Aono, "Single atom manipulation on the Si(111)7x7 surface by the scanning tunneling microscope (STM)", *Surface Science*, Vols. 287/288, pp. 1056-1061, 1993.

[21] B. Vikramaditya and B. J. Nelson, "Visually guided microassembly using optical microscopes and active vision", *Proc. IEEE Int'l Conf. on Robotics & Automation*, Albuquerque, NM, pp. 3172-3177, April 21-27, 1997.

[22] J. S. Villarrubia, "Morphological estimation of tip geometry for scanned probe microscopy", *Surface Science*, Vol. 321, No. 3, pp. 287-300, 1994.

[23] M. F. Yu *et al.*, "Three dimensional manipulation of carbon nanotubes under a scanning electron microscope", *Nanotechnology*, Vol. 10, No. 3, pp. 244-252, September 1999.